

Exact solutions of a class of $S=1$ quantum Ising spin models

Zhi-Hua Yang,¹ Li-Ping Yang,² Hai-Na Wu,³ Jianhui Dai,¹ and Tao Xiang^{2,4}

¹Zhejiang Institute of Modern Physics, Zhejiang University, Hangzhou 310027, China

²Institute of Theoretical Physics, Chinese Academy of Science, P.O. Box 2735, Beijing 100080, China

³College of Science, Northeastern University, Shenyang 110006, China

⁴Institute of Physics, Chinese Academy of Sciences, P.O. Box 603, Beijing 100080, China

(Received 17 November 2008; revised manuscript received 14 April 2009; published 23 June 2009)

We propose a hole decomposition scheme to exactly solve a class of spin-1 quantum Ising models with transverse or longitudinal single-ion anisotropy. In this scheme, the spin-1 model is mapped onto a family of the $S=1/2$ transverse Ising models, characterized by the total number of holes. A recursion formula is derived for the partition function based on the reduced $S=1/2$ Ising model. This simplifies greatly the summation over all the hole configurations. It allows the thermodynamic quantities to be rigorously determined in the thermodynamic limit. The ground-state phase diagram is determined for both the uniform and dimerized spin chains. The corresponding thermodynamic properties are calculated and discussed.

DOI: [10.1103/PhysRevB.79.214427](https://doi.org/10.1103/PhysRevB.79.214427)

PACS number(s): 75.10.Pq, 02.30.Ik, 75.10.Dg

I. INTRODUCTION

The phase transition driven by quantum fluctuations is one of the fundamental issues in quantum many-body systems. A number of novel phenomena associated with the transition such as the quantum critical behavior has been observed in a variety of condensed matter materials.^{1,2} One of the prototype model systems exhibiting the quantum phase transition is the one-dimensional (1D) spin-1/2 Ising lattice with a transverse field, namely the transverse Ising model (TIM),³⁻⁵ defined by

$$H_{\text{TIM}} = - \sum_j (JS_j^z S_{j+1}^z - hS_j^x), \quad (1)$$

where \vec{S}_j is the spin operator at the site j on a one-dimensional lattice of length L . The transverse field h introduces quantum fluctuation to the system, leading to a quantum phase transition from the ferromagnetic/antiferromagnetic-ordered states to the paramagnetic-disordered states above a critical value $h_c = J/2$. Actually the model is equivalent to a free spinless fermion system and can be exactly solved by applying the Jordan-Wigner transformation.^{6,7} Based on the exact solution, all physical quantities including the ground-state energy, the low-energy excitations, the specific heat, and other thermodynamic functions can be evaluated. This provides a thorough understanding of the quantum critical behavior of this system.

However, in real materials, the moments of atoms may be larger than 1/2. Despite immense efforts in the past three decades it is still very difficult to find exact solutions of the $S=1$ or other higher spin quantum Ising systems. This is partly due to the existence of the spin-neutral states $S^z=0$ (referred to as holes hereafter) in addition to the two spin-polarized states $S^z = \pm 1$ at each site in the $S=1$ spin chain. In these models, a hole can decay into a pair of spin-polarized states and vice versa, thus rendering the Jordan-Wigner approach invalid in exactly solving the $S=1$ TIM.

In this paper, we study a class of one-dimensional $S=1$ quantum Ising model (QIM) defined by the following Hamiltonian:

$$H = - \sum_j (J_j S_j^z S_{j+1}^z + f_j), \quad (2)$$

where $f_j = D_j^x (S_j^x)^2 + D_j^y (S_j^y)^2 + D_j^z (S_j^z)^2$ is the single-ion anisotropy term with site-dependent D_j^α ($\alpha=x, y, z$).

The above model has a classical limit where $D_j^x = D_j^y$. This corresponds to the Blume-Capel model.⁸ So the present model can be regarded as the quantum generalization of the Blume-Capel model. The simplest quantum case is the uniform chain defined by⁹

$$H_{\text{QIM}} = - \sum_j [JS_j^z S_{j+1}^z + D(S_j^x)^2]. \quad (3)$$

In two or higher dimensions, this kind of quantum Ising model with single-ion anisotropy was studied by a number of authors, based mainly on the mean-field approximations.^{10,11} In particular, the ground state of model (3) was shown to be equivalent to the $S=1/2$ TIM defined by Eq. (1).¹² Such equivalence is also valid for quantum Ising models with bond and site alternations¹³ or geometrical frustrations such as a fully frustrated spin-1 Ising delta chain.¹⁴

The purpose of the present paper is to study the physical properties of the model described by Eq. (2) based on the exact solution. The key idea in solving the proposed $S=1$ model is to divide the total Hilbert space of the $S=1$ system into a number of subspaces labeled by the number of holes. This is what we call the hole decomposition scheme (HDS). This HDS was developed in our recent work,⁹ where a recursion approach based on the HDS is suggested for the uniform chain. In the present paper, we give more comprehensive investigations for various properties of the $S=1$ model, including the case with dimerization.¹⁵ In particular, we show that for a given hole configuration, each sublattice system with purely polarized spins can be exactly solved in that case. Based on the exact solution we study how the quantum phase transitions and thermodynamic properties are affected by the interplay between the dimerization and the single-ion anisotropy. Depending on the strength of dimerization, we

find that the system undergoes a quantum phase transition where the criticality is the same as that of the uniform $S=1/2$ TIM.

We note that the spin-1/2 TIM can be realized in certain low-dimensional magnetic materials.^{16,17} For the systems with local moments larger than 1/2, the single-ion anisotropy generated by crystal fields and the dimerization may also become important.¹⁸ The $S=1$ TIM with the crystal-field splitting was used to describe the ferroelectric transition in SrTiO_3 .¹⁹ In a class of quasi-one-dimensional spin chains such as $[\text{Ni}_2(\text{Medpt})_2(\nu\text{-ox})(\text{H}_2\text{O})_2](\text{ClO}_4)_2 \cdot \text{H}_2\text{O}$, the magnetic Ni^{2+} ion shows not only a single-ion anisotropy^{20,21} but also a $S=1$ bond-alternating pattern, where Medpt is the bis(3-aminopropyl) methylamine.^{22,23} Recently, cold atoms or polar molecules in optic lattices were shown to be ideal systems to realize various quantum spin models.²⁴ In particular, the spin-1 models can be implemented by trapping polar molecules where the spin degrees of freedom can be described by the hyperfine vibrational states.²⁵

This paper is organized as follows. In Secs. II and III, we discuss some general properties of the model and introduce the HDS. In Sec. IV, we solve exactly the Hamiltonian in the presence of dimerization. In Sec. V, we study the low-energy excitation spectra and quantum phase transitions based on the exact solutions. In Sec. VI, we discuss in detail the recursion method introduced in Ref. 9 for evaluating thermodynamic quantities. Finally, we give a summary in Sec. VII.

II. HOLE DECOMPOSITION SCHEME

Let us consider a $S=1$ Ising lattice with single-ion anisotropy, defined by Eq. (2). (S_j^x, S_j^y, S_j^z) are the $S=1$ spin operators at lattice site $j=1, 2, \dots, L$, with the lattice length L . The uniform classical Blume-Capel model⁸ corresponds to the symmetric case with $D_j^x=D_j^y=D$. Because only two of these D_j^α terms are independent, we shall mainly consider the quantum case with $D_j^x=D_j$ and $D_j^y=D_j^z=0$, without losing generality. The case with $D_j^z \neq 0$ will be discussed later. We shall mainly focus on the dimerization case where

$$J_{2j-1}=J_1, \quad J_{2j}=J_2, \quad D_{2j-1}=D_1, \quad D_{2j}=D_2. \quad (4)$$

By definition, one has $(S_j^x)^2 = \frac{1}{4}(S_j^+S_j^+ + S_j^-S_j^- + S_j^+S_j^- + S_j^-S_j^+)$. So it is straightforward to show that $(S_j^x)^2$ does not couple $S_j^z=0$ state to $S_j^z=\pm 1$ states. Thus $(S_j^x)^2$ commutes with $(S_j^z)^2$. This leads to the following theorem

A. Theorem 1

When $S=1$, the total hole number operator $\hat{N}_0=L - \sum_{j=1}^L (S_j^z)^2$ commutes with the Hamiltonian for any site-dependent J_j and D_j

$$[\hat{N}_0, H]=0. \quad (5)$$

It means that the total number of holes is a conserved quantity if $S=1$. Consequently, the eigenstates of H can be classified by the eigenvalue p of \hat{N}_0 . In the discussion below, we will call the subsystem with p holes as the p th sector. Let \mathcal{H}_p be the Hilbert space of the p th sector, the total Hilbert

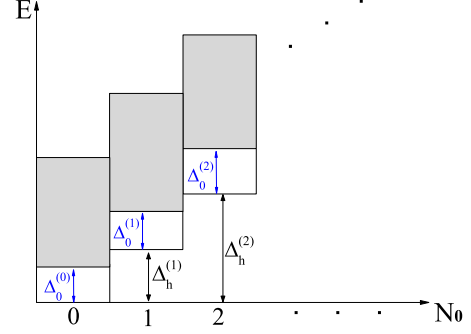


FIG. 1. (Color online) The schematic of the energy-band hierarchy. The boxes represent the subbands of the corresponding p th sector. $\Delta_0^{(p)}$ and $\Delta_h^{(p)}$ are the minimal gaps for the fermionic and hole excitations, respectively, in the p th sector. Several explicit results of these gaps are given in Sec. IV.

space is then given by the sum of all the subspaces

$$\mathcal{H} = \mathcal{H}_0 \oplus \mathcal{H}_1 \oplus \dots \oplus \mathcal{H}_L. \quad (6)$$

A complete set of the eigenstates in the p th sector forms a subband of the whole spectrum. Generally the lowest eigenenergy of the p th sector satisfies the following theorem

B. Theorem 2

Let $E(p, L)$ be the eigenenergy, corresponding to the eigenstate $|p, L\rangle$ of H , and $E_0(p, L)$ be the lowest eigenenergy in the p th sector, then the following inequality holds

$$E_0(p, L) < E_0(p+1, L). \quad (7)$$

This relationship is an extension of the Lieb-Mattis theorem derived initially for the uniform systems with ferromagnetic Ising couplings.²⁶ It still holds no matter whether the Ising couplings are ferromagnetic or antiferromagnetic. It indicates that in the absence of the D_j^z term, the ground state always lies in the $p=0$ sector and the energy spectrum of the system has a hierarchical structure.

There are two kinds of excitations in the system. One is the fermionic excitation within a given sector. The corresponding excitation energy is defined by $E(p, L) - E_0(p, L)$. The other is the hole excitation and the excitation energy with respect to the ground state is given by $E(p, L) - E_0(0, L)$. There are two kinds of minimal excitation gaps corresponding to these excitations

$$\Delta_0^{(p)} \equiv E_1(p, L) - E_0(p, L),$$

$$\Delta_h^{(p)} \equiv E_0(p, L) - E_0(0, L). \quad (8)$$

Figure 1 shows schematically the hierarchical band structure of the system. Within each band (or each box shown in Fig. 1) there are fermionic excitations, with minimal gaps $\Delta_0^{(p)}$. While the minimal gaps of the hole excitations $\Delta_h^{(p)}$ increase with p when the longitudinal anisotropy $D_j^z=0$.

III. MAPPING ONTO THE SPIN-1/2 TIM'S

The eigenstates of the Hamiltonian (2) can be generally expressed as $|\Psi\rangle = \sum_{m_j} F_{m_1, m_2, \dots, m_L} |m_1, m_2, \dots, m_L\rangle$, with

F_{m_1, m_2, \dots, m_L} being the wave function. As the total spin and its z component are not conserved, the summation runs over all $m_j=0, \pm 1$ states. However, by theorem 1, the local holes are good quantum numbers and can be regarded as nonmagnetic local impurities embedded in the $S=1/2$ Ising system. Assuming in the p th sector the holes are located at x_n ($n=1, 2, \dots, p$), then the corresponding eigenstates can be expressed as $|\Psi_{(p)}\rangle = \sum_{\tilde{m}_j} F_{\tilde{m}_1, \tilde{m}_2, \dots, \tilde{m}_L}^{(p)} \prod_{j=1}^L \otimes |\tilde{m}_j\rangle$, where $\tilde{m}_j = \pm 1$ if $j \neq x_n$ and $\tilde{m}_{x_n} = 0$.

In the $p=0$ sector, there are only two spin states at each site, corresponding to $\tilde{m}_j = \pm 1$, respectively. They are in one-to-one correspondence with the states of the spin-1/2 (Pauli) operators σ_j^z : $S_j^z |\tilde{m}_j\rangle \Leftrightarrow \sigma_j^z |\tilde{m}_j\rangle = \tilde{m}_j |\tilde{m}_j\rangle$. One has then the mapping relationship $S_j^\pm S_j^\pm \Rightarrow 2\sigma_j^\pm$, $S_j^\pm S_j^\mp - 1 \Rightarrow \pm \sigma_j^z$. Thus, $(S_j^z)^2$ acts like $(1 + \sigma_j^z)/2$. The original Hamiltonian, when acting on the $p=0$ subspace, has the following reduced form

$$H_{(0,L)} = - \sum_j J_j \sigma_j^z \sigma_{j+1}^z - \frac{1}{2} \sum_j D_j (1 + \sigma_j^z). \quad (9)$$

This is just the spin-1/2 Ising model with bond (site)-dependent Ising couplings and transverse fields.

Now let us turn to the $p=1$ sector. If the hole is located at the site x_1 , the corresponding state can be written as $|\Psi_{(1)}\rangle = \sum_{\tilde{m}_j} F_{\dots, \tilde{m}_{x_1-1}, 0, \tilde{m}_{x_1+1}, \dots}^{(1)} |\tilde{m}_1 \dots \tilde{m}_{x_1-1} 0_{x_1} \tilde{m}_{x_1+1} \dots \tilde{m}_L\rangle$. Now because the bonds connecting the hole are broken, the reduced Hamiltonian, obtained by acting the original one on the $p=1$ sector, is given by

$$H_{(1,L)} = H'_{(0,x_1-1)} + H'_{(0,L-x_1)} - D_{x_1}, \quad (10)$$

where $H'_{(0,l)}$ is the Hamiltonian of the spin-1/2 TIM segment of lengths l imposed by the open boundary condition. If $|\psi'(x_1-1)\rangle$ and $|\psi'(L-x_1)\rangle$ are the eigenstates of the segments $H'_{(0,x_1-1)}$ and $H'_{(0,L-x_1)}$, respectively, then

$$|\Psi_{(1)}\rangle = |\psi(x_1-1)\rangle \otimes |0_{x_1}\rangle \otimes |\psi(L-x_1)\rangle \quad (11)$$

is the eigenstate of $H_{(1,L)}$. This HDS can be easily generalized to the multihole sectors. For instance, the reduced Hamiltonian in a p -hole sector is given by

$$H_{(p,L)} = H'_{(0,x_1-1)} + H'_{(0,x_2-x_1-1)} + \dots + H'_{(0,L-x_p)} - \sum_{n=1}^p D_{x_n}, \quad (12)$$

where x_n 's are the positions of holes. Similarly, the eigenstate of $H_{(p,L)}$ can then be expressed in terms of those of the individual segments.

Therefore, all the eigenstates of the $S=1$ QIM [Eq. (2)] can be obtained by solving a set of the spin-1/2 TIMs. For the p th sector, the number of the $S=1/2$ TIM segments are $p+1$ or p , depending on whether the original chain is periodic or open. Note that the hole positions may vary along the chain, so there are many different hole configurations in a given sector. The decomposition of the total Hilbert space into the sum of subspaces can be formally represented by $[2 \oplus \mathbf{1}]^{\otimes L} = \mathbf{2}^{\otimes L} \oplus \mathbf{2}^{\otimes(L-1)} \otimes \mathbf{1} \oplus \mathbf{2}^{\otimes(L-2)} \otimes \mathbf{1}^{\otimes 2} \oplus \dots \oplus \mathbf{1}^{\otimes L}$, where the dimension of the $S=1$ system is given by $\dim \mathcal{H} = (2+1)^L = \sum_{p=0}^L 2^{L-p} C_p^L = \sum_{p=0}^L \dim \mathcal{H}_p$.

IV. DIMERIZED SPIN CHAIN

A. Nonhole sector

In this section, we follow the standard approach introduced in Refs. 6 and 27 to diagonalize the $p=0$ sector of the $S=1$ model [Eq. (9)]. We introduce the fermion operators c_j and c_j^\dagger and use the Jordan-Wigner transformation to rewrite Eq. (9) as follows:

$$H_{(0,L)} = \sum_{j,q} \left[c_j^\dagger A_{jq} c_q + \frac{1}{2} (c_j^\dagger B_{jq} c_q^\dagger - c_j B_{jq} c_q) \right] + H_{PB}, \quad (13)$$

where $H_{PB} = J_L (c_L^\dagger c_1^\dagger + c_L^\dagger c_1 - c_L c_1^\dagger - c_L c_1) (K_{L+1} + 1)$, $A_{jq} = A_{qj} = -D_j \delta_{j,q} - J_j \delta_{j+1,q} - J_{j-1} \delta_{j-1,q}$, and $B_{jq} = -B_{qj} = -J_j \delta_{j+1,q} + J_{j-1} \delta_{j-1,q}$. Notice that H_{PB} is the boundary term (which disappears for the open chains) and can be neglected in the thermodynamics limit.

Next, we introduce the Bogoliubov transformation as in the following:

$$\eta_k = \sum_j (g_{kj} c_j + h_{kj} c_j^\dagger); \quad \eta_k^\dagger = \sum_j (g_{kj}^* c_j^\dagger + h_{kj}^* c_j), \quad (14)$$

where, η_k and η_k^\dagger are the fermionic quasiparticle operators with quasimomentum k . They satisfy the usual anticommutation relations. While g_{kj} and h_{kj} are coefficient matrices which should be complex in general. Then, $H_{(0,L)}$ becomes

$$H_{(0,L)} = \sum_k \Lambda(k) \eta_k^\dagger \eta_k + \frac{1}{2} \sum_j A_{jj} - \frac{1}{2} \sum_k \Lambda(k). \quad (15)$$

If we define $(\Phi_k)_j = g_{kj} + h_{kj}$ and $(\Psi_k)_j = g_{kj} - h_{kj}$, the eigenvalue $\Lambda(k)$ can be solved by

$$M_{jq} (\Phi_k)_q = \Lambda^2(k) (\Phi_k)_j; \quad M_{jq} (\Psi_k)_q = \Lambda^2(k) (\Psi_k)_j, \quad (16)$$

with M being a symmetric matrix defined by $M = (A - B)(A + B)$, or $M_{jq} = (D_j D_q + 4J_{j-1} J_{q-1}) \delta_{j,q} + 2D_q J_{j-1} \delta_{j-1,q} + 2D_j J_{q-1} \delta_{j,q-1}$. For the dimerized (or alternating) chain, the M matrix depends on the boundary conditions and the parity of the chain length (even or odd). For simplicity, we here consider the case of periodic chain with even L , where

$$M = \begin{pmatrix} a_1 & b_1 & 0 & \dots & 0 & b_2 \\ b_1 & a_2 & b_2 & \dots & 0 & 0 \\ 0 & b_2 & a_1 & \dots & 0 & 0 \\ \dots & \dots & \dots & \dots & \dots & \dots \\ 0 & 0 & 0 & \dots & a_1 & b_1 \\ b_2 & 0 & 0 & \dots & b_1 & a_2 \end{pmatrix}, \quad (17)$$

with $a_1 = D_1^2 + 4J_2^2$, $b_1 = 2D_1 J_1$, $a_2 = D_2^2 + 4J_1^2$, and $b_2 = 2D_2 J_2$.

In order to solve Eq. (16) with this M matrix, we employ the following Ansatz:

$$(\Phi_k)_{2j} = A_e \exp[ik(2j)],$$

$$(\Phi_k)_{2j+1} = A_o \exp[ik(2j+1)]. \quad (18)$$

The ratio $\tau = A_o/A_e$ is then a measure of dimerization, determined by

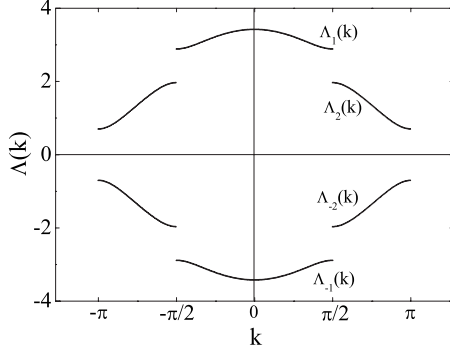


FIG. 2. The representative fermionic excitation spectra in the nonhole sector of the $S=1$ QIM with $Q>0$, $J_1=1.01$, $J_2=1$, $D_1=1.82$, and $D_2=0.9$. This kind of excitation for a sector with fixed hole number is similar though the quasimomentum is determined by the corresponding secular equation.

$$\tau = \frac{a_1 - a_2 \pm W}{2[b_1 e^{-ik} + b_2 e^{ik}]}, \quad (19)$$

where

$$W \equiv \sqrt{(a_2 - a_1)^2 + 4(b_1 - b_2)^2 + 16b_1 b_2 \cos^2 k}. \quad (20)$$

Note that when $a_1=a_2$ and $b_1=b_2$, we have $\tau = \pm 1$, as it should be for the uniform chain.

The eigenvalue $\Lambda^2(k)$ is then obtained by $\Lambda^2(k) = \Gamma^2 \pm \frac{W}{2}$, so that one has four branches of quasiparticle excitations

$$\Lambda_{\pm r}(k) = \pm \Gamma \sqrt{1 - (-1)^r \sqrt{1 - P + Q \cos 2k}}, \quad (21)$$

with $r=1, 2$, $\Gamma^2 = \frac{1}{2}(D_1^2 + D_2^2 + 4J_1^2 + 4J_2^2)$, $P\Gamma^4 = D_1^2 D_2^2 + 16J_1^2 J_2^2$, $Q\Gamma^4 = 8D_1 D_2 J_1 J_2$, and $k = 2\pi m/L$, ($m = -L/2, \dots, L/2 - 1$).

It should be noticed that $\Lambda_{\pm r}(k)$ (for $r=1, 2$) are invariants under the shift $k \rightarrow k + \pi$. Thus the quasimomentum k is constrained in one of the following regimes: (1) $k \in [-\pi/2, \pi/2)$ or (2) $k \in [-\pi, -\pi/2) \cup [\pi/2, \pi)$. Here we choose k to be in the first regime for $\Lambda_{\pm 1}(k)$ and in the second regime for $\Lambda_{\pm 2}(k)$. Figure 2 shows the typical energy dispersions for a dimerized system with $Q > 0$. The case with $Q < 0$ can be obtained by a reflection under the shift.

B. Single-hole sector

In the $p=1$ sector, the hole breaks the two bonds connected to it. For convenience, we assume that the hole is located at the site L . The reduced Hamiltonian can be rewritten as

$$H_{(1,L)} = H'_{(0,L-1)} - D_L, \quad (22)$$

where $H'_{(0,L-1)}$ is defined by Eq. (13) but with the open boundary conditions. The procedure for diagonalizing $H'_{(0,L-1)}$ is the same as for $H_{(0,L)}$. The eigenwave function is determined by Eq. (16) in a similar way. The only difference is that now the M matrix is a $(L-1) \times (L-1)$ matrix, with $M_{L-1,1} = M_{1,L-1} = 0$ and $M_{1,1} = a_0 (\equiv D_1^2)$.

Due to the open boundary condition, the Ansatz [Eq. (18)] is no longer valid. Intuitively, a reflection wave (e^{-ikj}) will be induced at the boundary in addition to the incoming wave

(e^{ikj}). Thus we suggest another Ansatz for the dimerized open chain as follows:

$$(\Phi_k)_{2j} = A_e (e^{2ikj} - t_e e^{-2ikj}),$$

$$(\Phi_k)_{2j+1} = A_o (e^{ik(2j+1)} - t_o e^{-ik(2j+1)}). \quad (23)$$

With this Ansatz, we find that τ and $\Lambda(k)$ take the same form as those defined in the $p=0$ case. The reflection coefficients, t_o and t_e , are given by

$$t_e = \frac{e^{iLk}}{e^{-iLk}}, \quad t_o = \frac{(b_1 e^{-ik} + b_2 e^{ik}) e^{iLk}}{(b_1 e^{ik} + b_2 e^{-ik}) e^{-iLk}}. \quad (24)$$

Moreover, the quasimomentum k is now determined by the following secular equation

$$\begin{aligned} & 2b_2[b_1^2 + b_2^2 + 2b_1 b_2 \cos 2k] \sin Lk \\ & = (a_0 - a_1)[b_1 \sin(L-2)k + b_2 \sin Lk] \\ & \quad \times [(a_1 - a_2) \pm W]. \end{aligned} \quad (25)$$

The equation is symmetric under $k \rightarrow -k$, thus we only need to solve the complex or positive k 's. The solution can be further simplified if $b_1=b_2$ (or $D_1 J_1 = D_2 J_2$) where $t_o = t_e$.

C. Multihole sectors

The previous approach is extended to the subsystems or sectors with more holes. The holes break the Ising couplings, leading to a series of segments of the spin-1/2 TIM's. For the periodic chain, the number of these segments is equal to the number of p holes (including the segment of zero length). If the holes are located at (x_1, x_2, \dots, x_p) , then the corresponding reduced Hamiltonian is given by Eq. (9), i.e., $H_{(p,L)} = \sum_{n=1}^p H'(0, l_n) - \sum_{n=1}^p D_{x_n}$, with $l_n = x_n - x_{n-1} - 1$ (where $x_0 = x_p - L$) being the length of the n th segment and

$$\begin{aligned} H'(0, l_n) = & - \sum_{j=x_{n-1}+1}^{x_n-2} J_{j,j+1} \sigma_j^z \sigma_{j+1}^z \\ & - \frac{1}{2} \sum_{j=x_{n-1}+1}^{x_n-1} D_j \sigma_j^x - \sum_{j=x_{n-1}+1}^{x_n-1} \frac{D_j}{2}. \end{aligned} \quad (26)$$

Each segment Hamiltonian $H'(0, l_n)$ can be diagonalized as $H'(0, l_n) = \sum_k \Lambda(k) (\eta_k^\dagger \eta_k - \frac{1}{2}) - \sum_{j=x_{n-1}+1}^{x_n-1} \frac{D_j}{2}$, where k is the quasimomentum satisfying the secular equation [Eq. (25)] (by replacing L by l_n). Notice that associated with the fixed length of the segment there are four different kinds of configurations, depending on whether the two edge holes are located at odd or even sites.

V. LOW ENERGY SPECTRA

A. Fermionic excitations in the nonhole sector

In the previous section, we show how to diagonalize the reduced Hamiltonians of different sectors. In a given hole sector, there are four branches of quasiparticle excitations, given by Eq. (21). Obviously, the two negative branches $\Lambda_{-r}(k)$ ($r=1, 2$) will be filled in the ground state of that sector.

In the $p=0$ sector, the ground state is given by $|\psi_0\rangle = \prod_{kk'} \eta_{-1,k}^\dagger \eta_{-2,k'}^\dagger |0\rangle$, where $\eta_{-r,k}^\dagger$ ($r=1,2$) are the fermionic quasiparticle operators in the branches $\Lambda_{-r}(k)$, k , and k' are the allowed momenta for $r=1,2$, respectively. The ground-state energy is given by $E_0(p=0,L) = \frac{1}{2} \sum_k \Lambda_{-1}(k) + \frac{1}{2} \sum_{k'} \Lambda_{-2}(k')$.

The low-energy excitations can be obtained by applying operators $\eta_{2,k'}^\dagger$ or $\eta_{-2,k'}$ on the ground state. The excitation energy is given by $\Lambda_2(k')$ [$=-\Lambda_{-2}(k')$]. When $Q>0$, the energy gap between the lowest excitation and the ground state is given by

$$\Delta_0 = \sqrt{\Gamma^2 - \sqrt{\Gamma^4 - \delta_-^4}}, \quad (27)$$

where $\delta_\pm = \sqrt{|D_1 D_2 \pm 4J_1 J_2|}$. If $|D_1| = |D_2| = |D|$ and $|J_1| = |J_2| = |J|$, one has $\Delta_0 = 2|J| \left| \frac{1}{|\lambda|} - 1 \right|$ with $\lambda = 2J/D$, reproducing the result of the uniform chain. In this case, the branches 1 and 2 connect smoothly. In the presence of dimerization, however, the two branches will split and produce a dimerization gap

$$\Delta_d = \frac{1}{2} (\sqrt{\Gamma^2 + \sqrt{\Gamma^4 - \delta_+^4}} - \sqrt{\Gamma^2 - \sqrt{\Gamma^4 - \delta_+^4}}). \quad (28)$$

B. Single-hole excitation

The ground state of the $p=1$ sector has L -fold degeneracy in the uniform chain, because the energy does not depend on the position of the hole. But in the presence of dimerization the degeneracy will be $L/2$ -fold. While the momentum dependence of the spectra can be determined as in the $p=0$ sector, the quasimomentum k must satisfy the secular equation associated with the open chain of length $L-1$.

In the lowest state of the $p=1$ sector, the bands with negative energies are fully filled. The corresponding energy is then given by $E_0(1,L) = \frac{1}{2} [\sum_k \Lambda_{-1}(k) + \sum_{k'} \Lambda_{-2}(k')] - \frac{1}{2} \max(D_1, D_2)$. The last term is contributed from the hole which may locate at either even or odd sites.

According to theorem 2, the ground state of the original Hamiltonian should be the one in the $p=0$ sector. So in addition to the fermionic excitations, inclusion of the $p=1$ sector (adding a hole to the system) will induce the hole excitations. The minimal hole excitation gap is given by $\Delta_h^{(1)} \equiv \Delta_h = E_0(1,L) - E_0(0,L)$. The typical behavior of Δ_h (as a function of D_2) is shown in Fig. 3 for fixed $J_1=10$, $D_1=2.0$, and $L=2000$, with either periodic or open boundary conditions.

In order to understand the difference in Δ_h for the periodic and open chains, we consider a special case where the chain is uniform and at the critical point, i.e., $D_1=D_2=D$, $J_1=J_2=J$, and $\lambda=2J/D=1$. In this simple case, the energy spectrum is given by $\Lambda(k) = -|D| \sqrt{1 + \lambda^2 + 2\lambda \cos k}$, and the allowed quasiparticle momenta are $k = \frac{2m\pi}{L}$ ($m = -L/2, \dots, L/2-1$) for the period boundary condition, and $k = \frac{2m\pi}{2L+1}$ ($m=1, \dots, L$) for the open boundary condition. Thus for sufficiently large L we obtain $\Delta_h \approx 0.136D$ and $\Delta_h \approx 0.318D$ for the open and periodic chains, respectively. Their difference, $\epsilon_s = 0.182D$, does not change for larger L . So it is the surface energy cost to turn into an open chain.

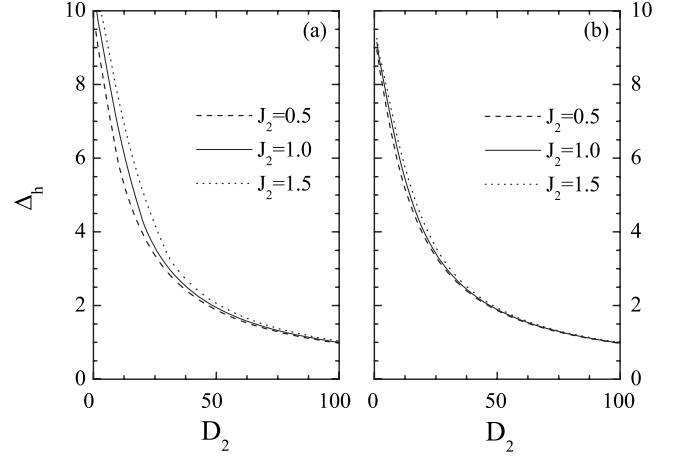


FIG. 3. The hole excitation gap Δ_h as a function of D_2 for the system with periodic (left panel) or open (right panel) boundary conditions. Three curves corresponding to $J_2=0.5, 1.0$, and 1.5 are plotted and $J_1=10$ and $D_1=2.0$ are fixed.

C. Multihole excitations

It is straightforward to extend the above discussion to a multihole system. Let us start with $p=2$. The eigenfunction in the $p=2$ sector is a direct product of the wave functions for the two $p=1$ segments, but with smaller lattice lengths $x-1$ and $L-x-1$, respectively, where $x \equiv x_2 - x_1$ is the distance between the two holes sited at x_1 and x_2 .

For the uniform chain, the lowest energy state of the $p=2$ sector should correspond to the configuration where two holes are close together, as in this case the total surface energy is minimized. So the lowest hole excitation gap in the $p=2$ sector is given by $\Delta_h^{(2)} = E_0(2,L) - E_0(0,L)$. For $p>2$, one can further show that the lowest state in the p th sector is the configuration in which all holes are close to each other. This is the hole condensation phase in one dimension. The remaining spin chain has a length $L-p$. When $p \ll L$ and $L \rightarrow \infty$, the finite-size effect is negligible so one has $\Delta_h^{(p)} \approx p\Delta_h$.

D. Phase diagram

We now discuss how dimerization influences the phase diagram. We have shown that the ground state still lies in the $p=0$ sector in the presence of dimerization. However, dimerization splits the bands and induces a gap at higher energies. The quantum critical points extend to lines, which are determined by the gapless condition, i.e., $\Delta_0=0$, or according to Eq. (27),

$$D_1 D_2 = \pm 4J_1 J_2. \quad (29)$$

The influence of dimerization can be seen more clearly by introducing (assuming $J_1 J_2 > 0$)

$$R = \frac{D_1 + D_2}{2\sqrt{J_1 J_2}}, \quad \Omega = \frac{D_1 - D_2}{2\sqrt{J_1 J_2}}, \quad (30)$$

where R describes the competition between D_j and J_j , and Ω is a measure of the dimerization strength. In the uniform

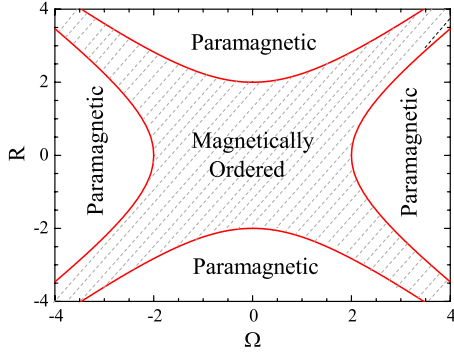


FIG. 4. (Color online) Ground-state phase diagram of the $S=1$ QIM. The Ω axis and R axis describe the dimerization strength and the competition parameter, see Eq. (30) in the main text. The dashed area is the magnetically ordered phase which extends slightly for small Ω but splits into two parts for $|\Omega| > 2$.

chain limit, $R=2/\lambda$ and $\Omega=0$. With increasing Ω , we have the following three situations: (1) in the weak dimerization regime, $|\Omega| < 2$, there is a pair of symmetric critical points, $\pm R_c$, with $R_c = \sqrt{\Omega^2 + 4}$. The ground state is magnetically ordered when $|R| < R_c$. (2) In the strong dimerization regime, $|\Omega| > 2$, there are two pairs of symmetric critical points, $\pm R_{c_1}$, $\pm R_{c_2}$, with $R_{c_1} = \sqrt{\Omega^2 + 4}$, $R_{c_2} = \sqrt{\Omega^2 - 4}$. The magnetically ordered phase appears when $R_{c_2} < R < R_{c_1}$. (3) when $|\Omega|=2$ ($R_{c_2}=0$), there are three critical points which take values $\pm 2\sqrt{2}, 0$, respectively. The ground state is magnetically disordered when $|R| > 2\sqrt{2}$ but ordered (either ferromagnetic or antiferromagnetic, depending on the signs of $J_{1,2}$) when $|R| < 2\sqrt{2}$. Note that the $R=0$ point corresponds to an alternating (or staggered) array of single-ion anisotropy ($D, -D, \dots, D, -D$). It becomes critical when $D = \pm 2\sqrt{J_1 J_2}$.

The $R-\Omega$ ground-state phase diagram is plotted in Fig. 4. The magnetically ordered phase and paramagnetic-disordered phase are separated by critical lines (red).

VI. THERMODYNAMIC PROPERTIES

In this section, we study the thermodynamic properties of the $S=1$ QIM. As was shown previously, this model is exactly solvable not only for the ground state, but also for all excited states. However, exactly evaluating the thermodynamic quantities is still a very hard task, particularly for large system size and dimerization. Here we shall develop the recursion method proposed in Ref. 9 in the evaluation of the partition function as well as other thermodynamic quantities for either uniform or dimerized chains.

A. Recursion method

Based on the HDS, the partition function $Z(L)$ of the system with lattice length L can be expressed as the sum of all the partition functions of the subsystems, i.e.,

$$Z(L) = \sum_{p=0}^L Z(p, L), \quad (31)$$

where $Z(p, L)$ is the partition function of the p th sector, because for fixed p , there are many different hole configura-

tions. So $Z(p, L)$ can be further rewritten as a sum over all possible hole configurations

$$Z(p, L) = \sum_{\{x_1, \dots, x_p\}} Z(x_1, \dots, x_p). \quad (32)$$

For each hole configuration $\{x_1, \dots, x_p\}$, the corresponding partition function of the open chain is given by ($\beta = 1/k_B T$)

$$Z(x_1, \dots, x_p) = \text{Tr} e^{[-\beta(\sum_{n=1}^{p+1} H'(0, l_n) - (1/2)\sum_{n=1}^p D_{x_n})]}, \quad (33)$$

where, $H'(l_n)$ is the Hamiltonian of the n th segment.

The partition functions of each segment can be regarded as the building blocks of total partition of the original system. These building blocks are denoted by $z(l_n)$, the partition functions of the spin-1/2 TIM segments with length l_n . Then, in the uniform case, $Z(L)$ can be expressed as $Z(L) = \sum_{p=0}^L \sum_{\{l_n\}} z(l_1) \alpha z(l_2) \alpha \dots \alpha z(l_{p+1})$, where $\alpha = \exp(\beta D/2)$ is the partition function of a hole, $z(1) = 2 \cosh(\beta D/2)$, and $z(0) \equiv 1$. As the length of the allowed segment may vary, one has the summation constraint $\sum_{n=1}^{p+1} l_n = L - p$. If we denote $Z^{(p)}(L-p) \equiv z(l_1) z(l_2) \dots z(l_{p+1})$, then the total partition function can be rewritten as

$$Z(L) = \sum_{p=0}^L \alpha^p Z^{(p)}(L-p), \quad (34)$$

where, α^p is contributed from the hole's.

To numerically evaluate the partition function, it is practically convenient to use the following recursion formula

$$Z^{(p)}(l) = \sum_{j=0}^l z(j) Z^{(p-1)}(l-j), \quad (35)$$

where, $Z^{(-1)}(l) \equiv \delta_{l,0}$ and $Z^{(0)}(l) \equiv z(l)$. By this way, we first calculate the building block, $z(l_n)$, and then by iterative use of above relation evaluate the partition function of the $S=1$ system. We find that this method is particularly efficient for the uniform chain, where the system size L could be as large as $L=10\,000$.

It is nontrivial to extend the above recursion method to the spin chain in the presence of dimerization. Here there are four kinds of blocks associated with the parity of the two ends. Thus we can denote them by $z_{r_1 r_2}(l_n)$, with $r_{1,2} (=o, e)$ indicating the left/right ends, respectively. The $S=1/2$ TIM segments with odd or even end sites can be solved exactly. The analytical expressions for $z_{r_1 r_2}(l_n)$ will be provided in a separated supplementary material.²⁸ In the following, we present some numerical results obtained by the recursion method while the system size is kept at $L=2000$. For simplicity, we use the open boundary condition for the original $S=1$ chain. The extension to the periodic boundary condition is straightforward.

B. Uniform spin chain

Thermodynamics quantities can be calculated from the partition function. In our model, an important physical quantity is the thermal average of the hole number, defined by

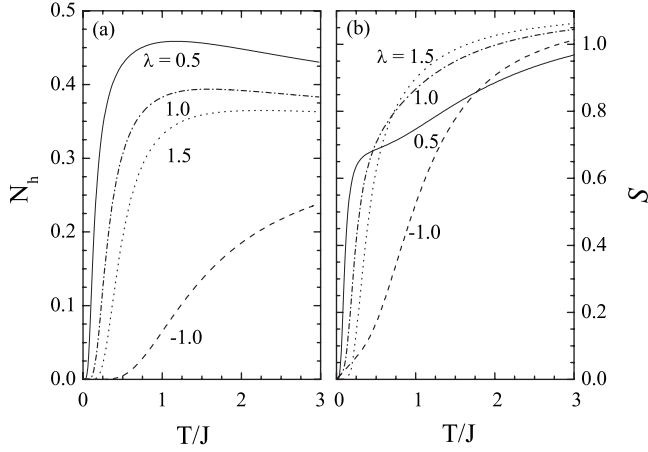


FIG. 5. (a) Temperature dependence of the hole concentration N_h and (b) the entropy S for a uniform spin chain with $\lambda = -1, 0.5, 1, 1.5$, respectively.

$$N_h = \frac{1}{Z(L)} \sum_{p=0}^L p \alpha^p Z^{(p)}(L-p). \quad (36)$$

Figure 5(a) shows the temperature dependence of N_h for several λ . At low temperatures, N_h increases rapidly with increasing temperature for small and positive λ . The proliferation of the hole number at low temperatures is obviously due to the smallness of the hole excitation gap. However, for the negative λ , say, $\lambda = -1$, the hole excitation gap is relatively larger, so N_h increases much slowly with temperatures.

Another interesting physical quantity is the entropy S , which we plot as a function of temperature for several different λ in Fig. 5(b). We find that the suppression of the entropy S is stronger for larger λ . The suppression is even more pronounced for the negative λ . These behaviors are similar to the temperature dependence of the hole number and are also due to the hole excitation gap.

We also find that the N_h approaches about $1/3$ in the high-temperature limit for all λ . Correspondingly, the entropy saturates at the value $\ln 3$ in the high-temperature limit (not fully shown in Fig. 5).

C. Dimerized spin chain

The recursion method, after some extensions discussed previously, is also used to evaluate thermodynamic quantities for a dimerized system. Figures 6 and 7(a) show the temperature dependence of the entropy S , the average hole concentration N_h , and the specific heat C in the ordered ($D_1 D_2 = J_1 J_2$), critical ($D_1 D_2 = 4 J_1 J_2$), and disordered phases ($D_1 D_2 = 16 J_1 J_2$), respectively. Here we fix $J_1 = 10$, $J_2 = 1$, and $D_1 = 2$, and choose several D_2 ($=5, 20$, and 80) in Figs. 6 and 7(a). Note that both the dimerization strength and competition parameter are tuned by varying D_2 . The general features of the hole number and the entropy are similar to that in the uniform case as the hole excitation gap plays the role at low temperatures (note that when $J_1 = 10$, $J_2 = 1$, and $D_1 = 2$, $\Delta_h = 7.450, 3.902$, and 1.202 for $D_2 = 5, 20$, and 80 , respectively).

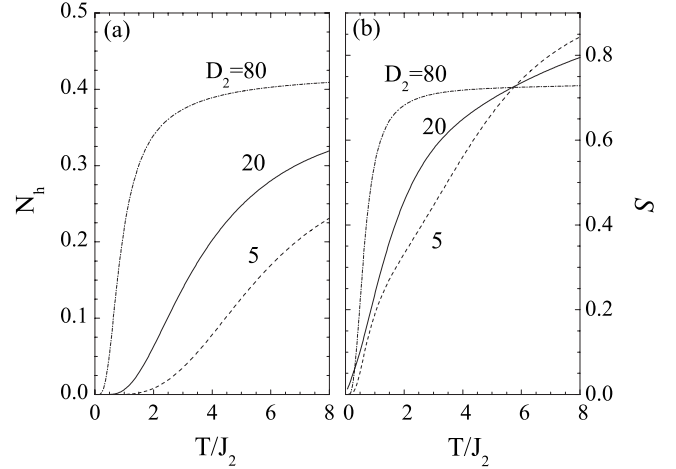


FIG. 6. (a) Temperature dependence of the hole concentration N_h and (b) the entropy S for a dimerized spin chain in three representative cases: $D_1 D_2 = J_1 J_2$ (dashed line), $4 J_1 J_2$ (real line), and $16 J_1 J_2$ (dash-dotted line), respectively, where, $J_1 = 10$, $J_2 = 1$, and $D_1 = 2$ are fixed.

In Fig. 7, the specific heat is plotted as a function of temperature in several cases. We find that at low temperatures the specific heat is peaked at the temperature scale near the hole excitation gap. The peak behavior changes depending on the competition of the fermionic and hole excitations. The influence of the dimerization on the specific heat can be clearly seen at relatively higher temperatures, as the dimerization-induced gap is much larger than the hole or fermion excitation gaps. Figure 7(b) shows the specific heats of the $S=1$ QIM system and its $p=0$ sector for the case $J_1 = 10$, $J_2 = 1$, $D_1 = 2$, $D_2 = 80$. Note that the $p=0$ sector is

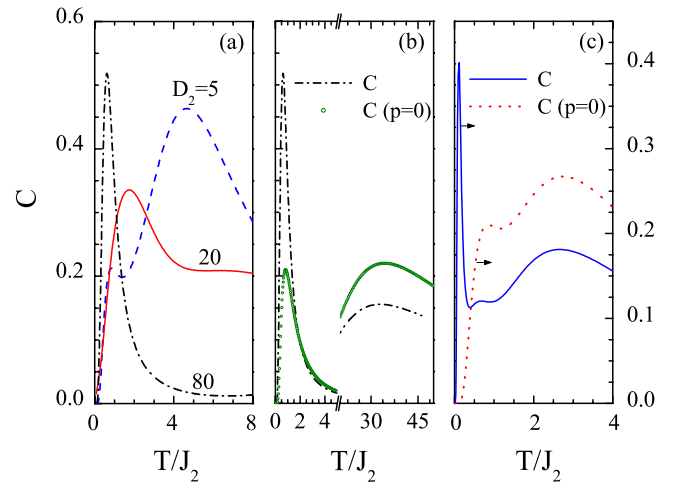


FIG. 7. (Color online) (a) The specific heat C for $D_1 D_2 = J_1 J_2$ and $D_2 = 5$ (blue-dashed line), $D_1 D_2 = 4 J_1 J_2$ and $D_2 = 20$ (red-real line), and $D_1 D_2 = 16 J_1 J_2$ and $D_2 = 80$ (dash-dotted line) with $J_1 = 10$, $J_2 = 1$, and $D_1 = 2$, respectively; (b) The specific heat C (dashed-dotted line) and the corresponding specific heat $C(p=0)$ for the $p=0$ subsystem (green open circle) for $D_1 D_2 = 16 J_1 J_2$ and $J_1 = 10$, $J_2 = 1$, $D_1 = 2$, and $D_2 = 80$, respectively. (c) The specific heat C (blue-real line) and $C(p=0)$ (red-dotted line) with $J_1 = J_2 = 1$, $D_1 = 2$, and $D_2 = 7$.

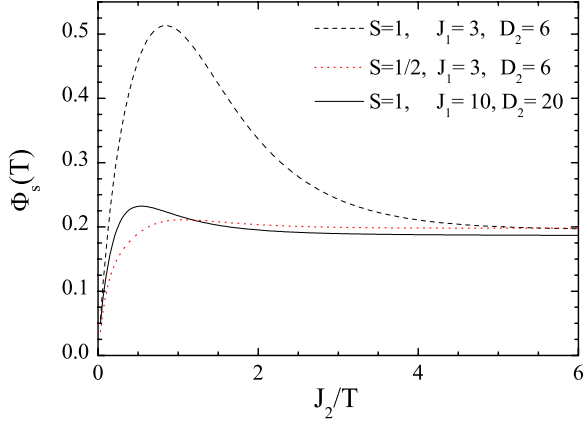


FIG. 8. (Color online) The scaled free energy for the dimerized systems in the quantum critical phase where $D_1 D_2 = 4J_1 J_2$. Two typical situations are plotted: ($J_2=3$ and $D_2=6$) and ($J_2=10$ and $D_2=20$) with small and large hole excitation gaps, respectively. Other parameters are $J_2=1$ and $D_1=2$. As a comparison, the corresponding $S=1/2$ TIM case is also plotted.

identical to the corresponding $S=1/2$ TIM. In this case $\Delta_0(\sim\Delta_h)$ is very small, leading to a sharp peak in the $S=1$ QIM system. We also find a well-separated and relatively round peak in the higher temperature regime where the energy scale is close to the dimerization gap $\Delta_d(=40.025)$.

The competitions among the dimerization effect, the hole excitations, and the fermion excitations can be seen more clearly from Fig. 7(c), where $J_1=J_2=1$, $D_1=2$, and $D_2=7$. In this case, the three kinds of gaps are well separated, $\Delta_h < \Delta_0 < \Delta_d$, so that the specific heat exhibits three peaks. The first one is a sharp peak around $T \sim \Delta_h$,²⁹ other two peaks are around $T \sim \Delta_0$ and $T \sim \Delta_d$, respectively. By contrast, the low-temperature sharp peak disappears in the $p=0$ sector and other two peaks still persist [see the red dotted line in Fig. 7(c)]. This is in agreement with the fact that no hole excitation exists in the $p=0$ sector.

We also calculated the scaled free energy $\Phi_s(T)$ at the critical point $D_1 D_2 = 4J_1 J_2$ for the dimerized spin chain. $\Phi_s(T)$ is defined by

$$\Phi_s(T) = \frac{2|J_2|[F(0) - F(T)]}{T^2}. \quad (37)$$

This quantity, which is identical to the specific-heat coefficient at low temperatures, was introduced in Ref. 30 in order to show the temperature persistence of the quantum critical scaling behavior in the $S=1/2$ TIM. The critical region, where quantum critical fluctuations dominate this quantity, should be a constant. It was shown that in the $S=1/2$ uniform TIM it deviates from the constant only when $T \geq J/2$, indicating a rather higher temperature scale below which the quantum critical scaling behavior persists.³⁰ In our recent work,⁹ we found that in the uniform $S=1$ QIM this behavior is strongly suppressed by the hole excitations. Here we find that the similar conclusion can be inferred in the presence of dimerization. In Fig. 8, we plotted the results for two cases (i) $J_1=3$, $J_2=1$, $D_1=2$, and $D_2=6$, and (ii) $J_1=10$, $J_2=1$, $D_1=2$, and $D_2=20$. As a comparison, the corresponding re-

sult for the dimerized $S=1/2$ TIM is also plotted. We find that the quantum critical scaling behavior at $T \rightarrow 0$ (or $J_2/T \rightarrow \infty$ in Fig. 8) persists approximately at finite $T \approx 0.5J_2$ for the dimerized $S=1/2$ TIM for case (ii) and at $T \approx 0.2J_2$ for case (i), respectively. This is because that the hole gap in case (i) is much smaller than case (ii). Consequently, the hole excitations play a more significant role in suppressing the quantum critical scaling behavior in the former case. This result is consistent with the conclusion in Ref. 9.

D. Hole condensations: The case with finite D_z

Now we turn to the case with nonzero D_z . It is straightforward to show that the D_z term plays the role of chemical potential for holes in the $S=1$ QIM.⁹ More specifically, the energy of a p -hole sector with finite D_z is related to that with $D_z=0$ by the following relationship [$E_0^{(p)}(0) \equiv E_0(p, L)$]

$$E_0^{(p)}(D_z) = E_0^{(p)}(0) + pD_z. \quad (38)$$

Thus, with finite D_z , the fermion excitation spectra remain unchanged, but the hole excitation gap becomes³¹

$$\Delta_h(D_z) = \Delta_h(0) + D_z. \quad (39)$$

Therefore, the ground state depends strongly on the value of D_z . When $D_z > -\Delta_h(0)$, the hole excitation is positive and the ground state is still in the $p=0$ sector. But when $D_z < -\Delta_h(0)$, the hole excitation gap is negative. This indicates that the $p=0$ sector is no longer the lowest energy state and there are holes in the ground state. As a result, theorem 2 is no longer valid in the present case. When L is sufficiently large and p is relatively small, the lowest energy of the p sector can be approximated by $E_0^{(p)}(0) \approx E_0^{(0)}(0) + p\Delta_h(0)$ as discussed in the previous section. Then, $E_0^{(p)}(D_z) \approx E_0^{(0)}(D_z) + p[\Delta_h(0) + D_z]$, so that we have

$$E_0^{(L)}(D_z) \leq \dots \leq E_0^{(1)}(D_z) \leq E_0^{(0)}(D_z). \quad (40)$$

Thus, the order of the band-structure hierarchy is completely overturned. In this case, the ground state is in the $p=L$ sector and all sites are occupied by holes.⁹ This can be also seen clearly from Fig. 9, where the temperature dependence of the hole concentration N_h is shown. We find that in the zero-temperature limit, N_h is equal to one when $D_z \leq -\Delta_h(0)$ or zero when $D_z > -\Delta_h(0)$.

VII. SUMMARY

In this paper, we have studied a class of exactly solvable $S=1$ QIMs with single-ion anisotropy. They exhibit a hierarchy of the band structure with both fermionic and hole excitations. The hole excitation gap can be tuned by the longitudinal crystal field D_z . It becomes zero when D_z is equal to $-\Delta_h(0)$. The ground state exhibits three distinct phases: the magnetically ordered or disordered phases when $D_z > -\Delta_h(0)$ or the hole condensation phase when $D_z < -\Delta_h(0)$. The transition to the hole condensation phase is of the first order.

We have shown that dimerization does not destroy the exact solvability of this model. To our knowledge, this is the first example in dimerized $S=1$ quantum spin systems where

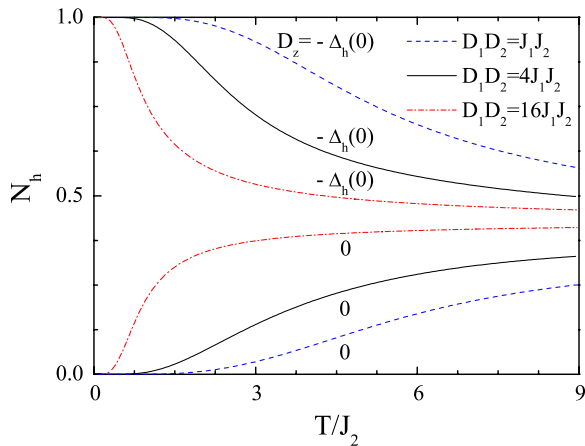


FIG. 9. (Color online) Temperature dependence of the hole concentration N_h for $D_z=0$ or $D_z=-\Delta_h(0)$. Other parameters are $J_1=10$, $J_2=1$, and $D_1=2$.

all the eigenstates as well as the wave functions and the eigenenergies can be solved exactly. The hole excitations enhance the thermodynamic fluctuations as evidenced in the specific heat which shows a sharp peak in the low-temperature region where the hole excitations proliferate. This strongly reduces the characteristic temperature below which the quantum criticality persists. All these results are

robust against the dimerization. However, dimerization deforms the phase diagram and affects the high-energy behavior.

We have developed a recursion method to sum over all hole configurations efficiently. This provides a powerful approach for evaluating rigorously all thermodynamic quantities as well as static and dynamic correlation functions of the QIMs in the thermodynamic limit. The detailed derivations for these quantities in the presence of dimerization will be provided as a supplementary material.²⁸ The recursion method holds not just for the model studied here. It can be easily extended and applied in other physical systems whose Hamiltonian can be written as a sum of independent spin segments separated by nonmagnetic impurities such as Pd-doped or Zn-doped quasi-one-dimensional antiferromagnets $\text{Sr}_2(\text{Cu}_{1-x}\text{Pd}_x)\text{O}_3$ or $\text{Cu}_{1-x}\text{Zn}_x\text{GeO}_3$.^{32,33}

ACKNOWLEDGMENTS

Z.H.Y. would like to thank Z. X. Xu for helpful discussions. This work was supported in part by the National Natural Science Foundation of China, the National Program for Basic Research of China, the PCSIRT (Grant No. IRT-0754), and SRFDP (Grant No. J20050335118) of the Education Ministry of China.

- ¹M. Greiner, O. Mandel, T. Esslinger, T. W. Hänsch, and I. Bloch, *Nature (London)* **415**, 39 (2002).
- ²P. Gegenwart, Q. Si, and F. Steglich, *Nat. Phys.* **4**, 186 (2008).
- ³S. L. Sondhi, S. M. Girvin, J. P. Carini, and D. Shahar, *Rev. Mod. Phys.* **69**, 315 (1997).
- ⁴S. Sachdev, *Quantum Phase Transitions* (Cambridge University Press, New York, 1999).
- ⁵B. K. Chakrabarti, A. Dutta, and P. Sen, *Quantum Ising Phase and Transitions in Transverse Ising Models* (Springer, Berlin, 1996).
- ⁶E. Lieb, T. Schultz, and D. Mattis, *Ann. Phys. (N.Y.)* **16**, 407 (1961).
- ⁷P. Pfeuty, *Ann. Phys. (N.Y.)* **57**, 79 (1970).
- ⁸M. Blume, *Phys. Rev.* **141**, 517 (1966); H. W. Capel, *Physica* **32**, 966 (1966).
- ⁹Z. H. Yang, L. P. Yang, J. Dai, and T. Xiang, *Phys. Rev. Lett.* **100**, 067203 (2008).
- ¹⁰X. F. Jiang, J. L. Li, J. L. Zhong, and C. Z. Yang, *Phys. Rev. B* **47**, 827 (1993).
- ¹¹N. C. Eddeqaqi, M. Saber, A. El-Atri, and M. Kerouad, *Physica A* **272**, 144 (1999).
- ¹²J. Oitmaa and A. M. A. von Brasch, *Phys. Rev. B* **67**, 172402 (2003).
- ¹³H. N. Wu, Z. H. Yang, J. Dai, and H. P. Ying, *Mod. Phys. Lett. A* **22**, 727 (2007).
- ¹⁴Y. Fukumoto and A. Oguchi, *Prog. Theor. Phys.* **115**, 847 (2006); Y. Fukumoto and A. Oguchi, in *Low Temperature Physics: 24th International Conference on Low Temperature Physics LT24*, AIP Conf. Proc. No. 850 (AIP, Melville, NY, 2006), p. 1081.

- ¹⁵While “dimerization” usually refers to the alternating antiferromagnetic coupling, here we use it to indicate that both the Ising coupling and the single-ion anisotropy can be of alternating pattern with period 2.
- ¹⁶J. Richter, S. E. Kruger, D. J. J. Farnell, and R. F. Bishop, *Series on Advances in Quantum Many-Body Theory Vol. 5* (World Scientific, Singapore, 2001), p. 239.
- ¹⁷D. Bitko, T. F. Rosenbaum, and G. Aeppli, *Phys. Rev. Lett.* **77**, 940 (1996).
- ¹⁸A. Abragam and B. Bleaney, *Electron Paramagnetic Resonance of Transition Ions* (Oxford University, Oxford, 1970).
- ¹⁹Y. Yamada, N. Todoroki, and S. Miyashita, *Phys. Rev. B* **69**, 024103 (2004).
- ²⁰A. Esucier, R. Vicente, X. Solans, and M. Font-Baidía, *Inorg. Chem.* **33**, 6007 (1993).
- ²¹J. J. Borrás-Almenar, E. Coronado, J. Curely, and R. Georges, *Inorg. Chem.* **34**, 2699 (1995).
- ²²S. Kimura, S. Hirai, Y. Narumi, K. Kindo, and M. Hagiwara, *Physica B* **294–295**, 47 (2001).
- ²³Y. Narumi, M. Hagiwara, R. Sato, K. Kindo, H. Nakano, and M. Takahashi, *Physica B* **246–247**, 509 (1998); Y. Narumi, R. Sato, K. Kindo, and M. Hagiwara, *J. Magn. Magn. Mater.* **177–181**, 685 (1998).
- ²⁴A. Micheli, G. K. Brennen, and P. Zoller, *Nat. Phys.* **2**, 341 (2006).
- ²⁵G. K. Brennen, A. Micheli, and P. Zoller, *New J. Phys.* **9**, 138 (2007).
- ²⁶E. Lieb and D. Mattis, *Phys. Rev.* **125**, 164 (1962).
- ²⁷T. D. Schultz, D. C. Mattis, and E. Lieb, *Rev. Mod. Phys.* **36**, 856 (1964).

²⁸See EPAPS Document No. E-PRBMDO-79-081921 about some details of the exact solutions, together with some additional discussions on the Green's functions, the spin-spin correlation functions, as well as the spin susceptibility. For more information on EPAPS, see <http://www.aip.org/pubservs/epaps.html>.

²⁹In the presence of dimerization the hole excitation gap is also dependent on the odd/even sites where the hole is located. Here we define the smaller one by Δ_h .

³⁰A. Kopp and S. Chakravarty, *Nat. Phys.* **1**, 53 (2005).

³¹In the following, we use $\Delta_h(0)$ to explicitly denote the hole excitation gap in the case with $D_z=0$, in order to distinguish the one with $D_z \neq 0$.

³²J. Sirker, N. Laflorencie, S. Fujimoto, S. Eggert, and I. Affleck, *Phys. Rev. Lett.* **98**, 137205 (2007).

³³M. Hase, I. Terasaki, Y. Sasago, K. Uchinokura, and H. Obara, *Phys. Rev. Lett.* **71**, 4059 (1993).